Journal of Integrative Agriculture 2025, 24(3): 966–983

Available online at ScienceDirect

Journal of Integrative Agriculture

RESEARCH ARTICLE

Ecological risks linked with ecosystem services in the upper reach of the Yellow River under global changes

Ruowei Li[1, 2], Jian Sun[1, 2#], Guodong Han[2#], Zixuan Qi[3], Yunhui Li[1], Junhe Chen[1], Wen He[4], Mengqi Zhang[1], Chaowei Han[5], Jieji Duo[1, 6]

[1] *State Key Laboratory of Tibetan Plateau Earth System Science (LATPES), Institute of Tibetan Plateau Research, Chinese Academy of Sciences, Beijing 100101, China*

[2] *Key Laboratory of Grassland Resources of the Ministry of Education, College of Grassland, Resources and Environment, Inner Mongolia Agricultural University, Hohhot 010019, China*

[3] *Guangdong Provincial Key Laboratory of Water Quality Improvement and Ecological Restoration for Watersheds, School of Ecology, Environment and Resources, Guangdong University of Technology, Guangzhou 510006, China*

[4] *Institute for Disaster Management and Reconstruction, Sichuan University–The Hong Kong Polytechnic University, Chengdu 610207, China*

[5] *Institute of Grassland Research, Chinese Academy of Agricultural Sciences, Hohhot 010010, China*

[6] *Haixi Forest Pest Control and Quarantine Center, Delingha 817099, China*

Highlights

- Ecological risks adversely affect ecosystem services in the upper reach of the Yellow River.
- Ecological risks continue to increase under different climate scenarios.
- Diverse managements can achieve sustainable development of the upper reach of the Yellow River.

Abstract

There is growing interest in introducing ecological risks (ERs) and ecosystem services (ESs) into environmental policies and practices. However, the integration of ESs and ERs into actual decision-making remains insufficient. We simulated the spatiotemporal dynamics of ESs (e.g., carbon storage, water yield, habitat quality, and soil conservation) and ERs in the upper reach of the Yellow River (URYR) from 2000 to 2100. Additionally, we explored their relationships by combining the InVEST model and a landscape ecological risk model with CMIP6 data. Our main findings showed that regional ERs change in response to land use and environmental dynamics. Specifically, the ER area decreased by 27,673 m^2 during 2000–2020, but it is projected to increase by 13,273, 438, and 68 m^2 under the SSP1-2.6, SSP2-4.5, and SSP5-8.5 scenarios, respectively. We also observed remarkable spatial differences in ESs and ERs between past and future scenarios. For instance, the source area of the URYR exhibited high ESs and low ERs (P<0.001), while the ESs and ERs are declining and increasing, respectively, in the northeastern URYR (P<0.05). Finally, we proposed a spatial optimization framework to improve ESs and reduce

Received 13 May, 2024 Accepted 19 August, 2024

Ruowei Li, Mobile: +86-18747794658, E-mail: liruowei199666@163.com; #Correspondence Jian Sun, Mobile: +86-18301068172, E-mail: sunjian@itpcas.ac.cn; Guodong Han, Mobile: +86-13087122590, E-mail: hanguodong@imau.edu.cn

doi: 10.1016/j.jia.2024.09.015

ERs, which will support regional sustainable development.

Keywords: climate change, CMIP6, Yellow River basin, Qinghai-Tibet Plateau, adaptive management, sustainable development

1. Introduction

The ecosystem provides abundant material resources for human beings, and plays crucial roles in climate regulation, habitat preservation, and soil and water conservation (Costanza *et al.* 1997; Sun and Shi 2020). Consequently, maintaining the structure, function, and services of ecosystems is fundamental for achieving sustainable development. Currently, climate change, the growing population, and urban expansion are widely recognized as the primary drivers of declines in ecosystem services (ESs) (Bryan *et al.* 2018; Cai *et al.* 2023; Huang *et al.* 2024), which further intensify ecological risks (ERs) (Wang *et al.* 2020; Mann *et al.* 2021).

Clarifying the linkages between ERs with ESs is vital for exploring effective ways to maintain ecosystem sustainability (Liu Y X *et al.* 2016; Cao *et al.* 2019). Nevertheless, numerous studies on ESs have focused on their trade-offs and synergies, as well as the spatiotemporal dynamics and divers (Maes *et al.* 2019; Zhou *et al.* 2019; Wang T *et al.* 2021; Jiang *et al.* 2023). Similarly, studies on ERs have concentrated on their evaluation and quantification, and understanding their spatial and temporal changes (Jiang *et al.* 2023). Although they are often treated as separate topics (Chen D S *et al.* 2021; Wang H *et al.* 2021), integrating ESs into the ER assessment framework is increasingly recognized as beneficial (Xing *et al.* 2020; Aneseyee *et al.* 2022). Specifically, the correlation, coupling, and coordination between ESs and ERs have been well explored (Zhang D H *et al.* 2022; Liu F L *et al.* 2023). The combined assessment of ESs and ERs can enhance the accuracy of regional management strategies (Li and Gao 2019; Xing *et al.* 2020; Sun M H *et al.* 2021). Importantly, both ESs and ERs are influenced by uncertain future factors such as climate change (Li C W *et al.* 2023), land use scenarios (Yang *et al.* 2020), policies (Lin *et al.* 2019), and socio-economic factors (Chen W X *et al.* 2021). Currently, the long-term evolutionary trends of regional ESs and ERs under global change remain unclear (Lin *et al.* 2021; Gao *et al.* 2022; Qi *et al.* 2023). Hence, projecting regional ES and ER dynamics under future climate changes and land use/cover changes (LUCC), especially in fragile ecosystem, is urgently needed (Cao *et al.* 2019; Zhang D H *et al.* 2022; Huang *et al.* 2023).

In the upper reach of the Yellow River (URYR), which includes national parks and key ecological functional areas such as the Qilian Mountains and the source of the Three Rivers, vital ESs are provided (Fan *et al.* 2020). In recent decades, the URYR has experienced remarkable variations in climate, geology, geomorphology, soil composition, vegetation patterns, and land use types (Fan *et al.* 2020). In the early 2000s, Water Conservancy Project and the Grain for Green Project led to revegetation, which significantly reduced the sediment in the Yellow River basin (Wang *et al.* 2016; Best 2019). However, under the influence of global changes, including climate warming, soil erosion, and vegetation destruction, the risk of flooding in the Yellow River basin is expected to increase over the next 20 years (Wang *et al.* 2016; Song *et al.* 2022). Meanwhile, overgrazing, unsustainable agricultural activities, and irrational land use also greatly impact the ESs and exacerbate ERs in the URYR (Liu L *et al.* 2016; Zhang *et al.* 2020). Addressing these concerns requires a comprehensive exploration of the basin's future trajectory and the dynamic shifts in its ESs and ERs, which is strategically vital for both ecological conservation and high-quality development (Zhang *et al.* 2024). Yet, few studies have investigated the consequences of current and future climate and land use changes in the URYR. Therefore, it is still challenging to implement practical and effective management that can simultaneously reduce ERs and enhance ESs (Bennett 2017; Hou *et al.* 2017; Islam *et al.* 2019; Wang Y *et al.* 2021).

In this study, we employed the InVEST model and a landscape ecological risk assessment model to simulate the evolution of ESs and ERs under the dynamics of climate change and LUCC. Our objectives were to: (1) evaluate the spatial distribution patterns of ESs and ERs in the URYR from 2000 to 2100, (2) clarify the dynamics and linkages between ESs and ERs, and (3) integrate ESs and ERs into the spatial planning of ecological functional areas by proposing targeted recommendations for future regional risk management. Overall, this study aims to illustrate how combining ESs and ERs can provide essential insights for managing, developing, and protecting the URYR and surrounding ecosystems from the increasing dual impacts of human activities and climate change.

2. Materials and methods

2.1. Study area

The URYR originates from the Bayinkara Mountains on the Qinghai-Tibet Plateau and flows through China's first and second terraces before reaching Hekou Town in Inner Mongolia, China (Fig. 1). The river is 3,472 km long, and the basin area covers 4.29×10^5 km^2 (Li B F *et al.* 2023). The climate in this region is complex and diverse, ranging from alpine and humid areas to arid desert regions. The mean annual temperatures range from –3°C to 7°C, and the mean annual precipitation is 379.7 mm, characteristic of a typical continental climate. Grassland ecosystems are widely distributed across Qinghai, Gansu, and Inner Mongolia of China, accounting for over 80% of current and future land use. Croplands are primarily distributed within the Hetao region of Inner Mongolia and western Qinghai Province. Similarly, urban areas are clustered around the croplands, such as in Lanzhou, Hohhot, Baotou, and Ordos, China. Meanwhile, the study area is rich in rivers, lakes, wetlands, and nature reserves, providing a variety of essential ESs (Chen *et al.* 2019). In recent years, climate change and human activities have threatened biodiversity, soil quality, carbon sequestration, and water conservation (Wang Y *et al.* 2021). Thus, assessing ESs and ERs is indispensable for ensuring regional ecological security in the URYR. The detailed research framework is shown in Fig. 2.

2.2. Data sources

Climate data The climate data used in this study included both observational and model scenario data. Observed meteorological records were provided and quality controlled by the China Meteorological Administration (https://www.cma.gov.cn/). Specifically, we employed daily meteorological data from 265 national weather stations in the URYR and surrounding areas, covering the period from 1961 to 2020. Biharmonic spline interpolation was then used to generate high-resolution (0.1°) daily precipitation and temperature datasets. Future meteorological data under different shared socioeconomic pathways (SSP) scenarios for 2020–2100 were obtained from the World Climate Research Program's Coupled Model Intercomparison Project Phase 6 (CMIP6) (https://esgf-node.llnl.gov/projects/cmip6). We selected three SSP scenarios in CMIP6 (SSP1-2.6, SSP2-4.5, and SSP5-8.5) according to different development paths, and these scenarios have been widely used to predict future regional development

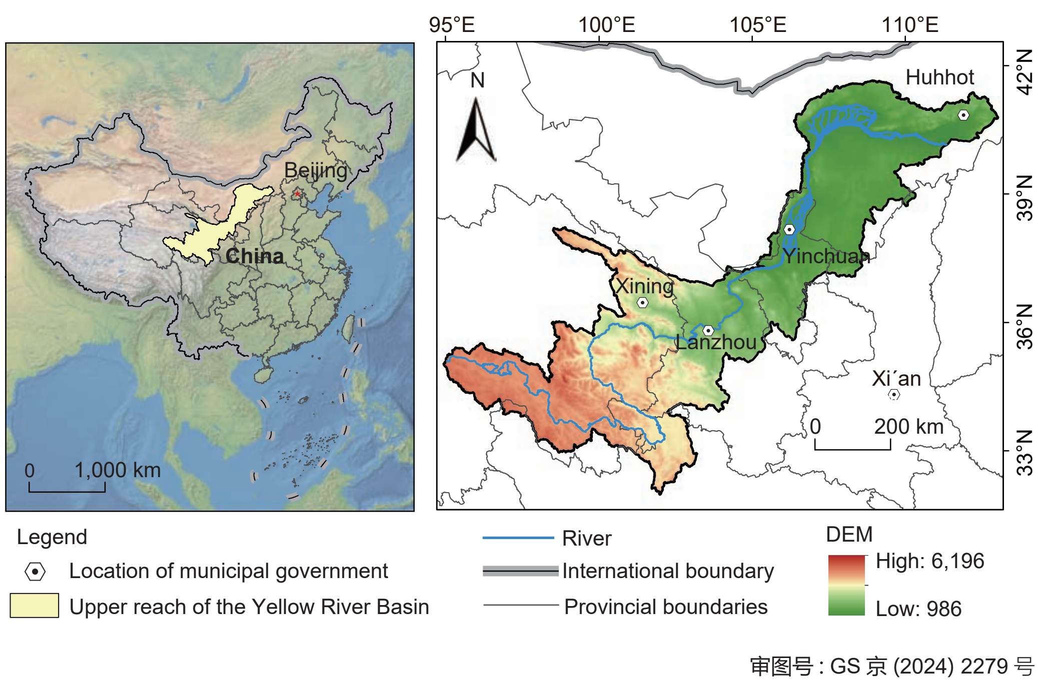

Fig. 1 Location of the upper reach of the Yellow River (URYR), China. The URYR originates from the Bayinkara Mountains on the Qinghai-Tibet Plateau and flows through Qinghai, Gansu and Ningxia before reaching Hekou Town in Inner Mongolia, China.

and climate change (Jiang and O'Neill 2017; Magalhães Filho *et al.* 2022) (Table 1). We chose three global models from CMIP6 that perform well in simulating future climatic conditions. Specifically, monthly minimum and maximum temperatures (°C) and solar radiation were needed to calculate evapotranspiration, which limited the number of CMIP6 models employed in this study. We also conducted a literature review on the performance of various CMIP6 models at the region scale and confirmed that these three models perform well in future climate simulations (Zhai *et al.* 2020; Qin *et al.* 2021; Su *et al.* 2021; Zhu *et al.* 2021; Ali *et al.* 2022; Li C *et al.* 2022; Lu *et al.* 2022) (Table 2).

Land use data The historical land use data (2000–2020) were obtained from the European Space Agency Climate Change Initiative (ESA-CCI; https://www.esa-landcover-cci.org/) at a spatial resolution of 300 m. The future land use demands under the three SSP scenarios were calculated using the LUH2 dataset (https://luh.umd.edu/) from the CMIP6 project. The two datasets were classified into six distinct categories: cropland, forest, grassland, barren, urban, and water, due to variations in the land classification systems between LUH2 (12 types) and ESA-CCI (22 types) (Qi *et al.* 2023, 2024). The classification methods and data processing procedures are presented in Appendices A and B.

Other data Digital elevation model (DEM), geographic data (e.g., vector data of administrative boundaries, cities, and rivers), and other relevant data were used to simulate and validate the InVEST model. The resolution of all raster data was standardized to 1 km using bilinear resampling in ArcGIS 10.6 (ESRI, Inc., Redlands, CA, USA). Additionally, the projection for all data was converted to the equal area projection of WGS1984 Albers to ensure spatial consistency across the multiple data sources. Data preprocessing primarily included cropping, splicing, and resampling. The data sources are listed in Table 3.

2.3. Methods

Climate data processing In this study, Delta downscaling was used to calibrate the output of the

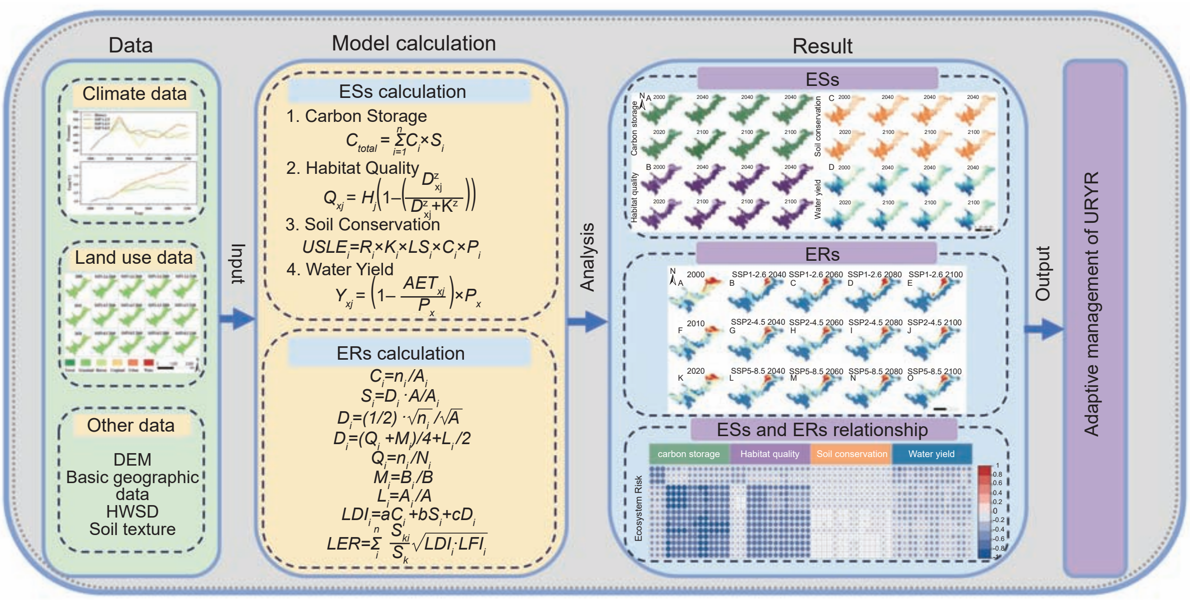

Fig. 2 The working flow chart of this study. DEM, digital elevation model; HWSD, Harmonized World Soil Database; ESs, ecosystem services; ERs, ecosystem risks; URYR, the upper reach of the Yellow River.

Table 1 Shared socioeconomic pathway (SSP) forcing scenarios under three representative concentration pathway (RCP) scenarios

SSP scenario	Pathway	Climate type (in 2100 forcing level; W m^{-2})	Scenario description
SSP1-2.6	Sustainability	2.6	Sustainability (the shift to sustainable practices, less than 2°C warming by 2100)
SSP2-4.5	Middle of the road	4.5	A central pathway (continuing historical patterns)
SSP5-8.5	Fossil fuel-driven development	8.5	Fossil fuel-driven development (an energy intensive, fossil fuel-based economy)

Table 2 Information of the CMIP6 models

Model	Institute	Country	Resolution (lon°×lat°)
ACCESS-ESM1-5	Commonwealth Scientific and Industrial Research Organization and Australian Research Council Centre of Excellence for Climate System Science	Australia	1.25°×1.875°
MRI-ESM2-0	Meteorological Research Institute, Ibaraki	Japan	1.125°×1.125°
NESM3	Nanjing University of Information Science and Technology	China	1.87°×1.87°

Table 3 Dataset sources

Data	Spatial resolution	Source
Digital elevation model (DEM)	250 m	http://www.resdc.cn
Basic geographic data (vector data of administrative boundaries, cities, and rivers)	Line/Point data	http://www.resdc.cn
Harmonized World Soil Database (HWSD)	1 km	https://westdc.westgis.ac.cn/
Reference crop evapotranspiration	1 km	http://www.geodata.cn
World soil dataset	1 km	https://www.crensed.ac.cn/portal/
Soil texture	1 km	http://www.resdc.cn
Carbon density	–	https://www.escience.org.cn/
Sub-basin boundaries	Line data	Hydrologic analysis tool in ArcMap software
Spatial dataset of ecosystem services in China	250 m	http://www.csdata.org/
Net primary productivity (NPP)	1 km	http://www.resdc.cn

different CMIP6 models, aiming to reduce the uncertainty of regional scale climate simulations and improve the data resolution (Qi *et al.* 2023, 2024). Using the Delta downscaling method, we generated future daily precipitation and temperature data at a resolution of 0.1° (Biharmonic spline interpolation) for the period from 2020 to 2100 (Moreno and Hasenauer 2016; Peng *et al.* 2018; Sun S *et al.* 2021). The calculation formulae are:

Precipitation:

$$(a)\frac{X_{m-n}}{\overline{X}_{a-n}}=E_{m-n}(b)E_{m-n}\rightarrow E'_{m-n}\times\overline{Z}_{a-n}=Y_{m-n} \quad (1)$$

Temperature:

$$(a)X_{m-n}-\overline{X}_{a-n}=E_{m-n}(b)E_{m-n}\rightarrow E'_{m-n}(c)E'_{m-n}\times\overline{Z}_{a-n}=Y_{m-n} \quad (2)$$

where X_{m-n} is the low spatial resolution long-term climate data, E_{m-n} is the residual value of low spatial resolution, E'_{m-n} is the high spatial resolution residual value, $\overline{Z}_{a-n}$ is the reference climate data with high spatial resolution and a long time series, and Y_{m-n} is the generated downscaling data. Among them, m is the sequence value of the annual time scale, n is the daily time scale sequence value, and a is the annual time scale sequence value of selected reference data.

Assessment of ecosystem services The URYR serves as an irreplaceable ecological barrier that provides critical services such as soil and water conservation, biodiversity protection, carbon storage, and other ecological functions (Guo *et al.* 2022). In this study, four key functions of the URYR, including carbon storage (CS), soil conservation (SC), water yield (WY), and habitat quality (HQ), were simulated using the InVEST model, following the methodology outlined previously (Li R W *et al.* 2023). Furthermore, SC in the URYR was evaluated through the sediment delivery module of the InVEST model, which calculates soil loss for each grid cell based on the universal soil loss equation. The calculation formulae are:

$$SC_i=RLKLS_i-USLE_i \quad (3)$$

$$RLKLS_i=R_i\times K_i\times LS_i \quad (4)$$

$$USLE_i=R_i\times K_i\times LS_i\times C_i\times P_i \quad (5)$$

where, SC_i is the soil retention of grid cell i (t km^{-2}); $RKLS_i$ is the potential soil erosion amount (t); $USLE_i$ is the actual amount of soil erosion (t); R_i is the precipitation erosion factor of the grid cell; K_i is the soil erodibility factor of the grid cell; LS_i is the slope length factor of the grid cell; C_i is the vegetation cover factor of the grid cell; and P_i is the soil protection measure factor of the grid unit (Lufafa *et al.* 2003).

Calculation of landscape ecological risks According to previous studies (Gong *et al.* 2015; Mo *et al.* 2017; Lin *et al.* 2019), the ERs were calculated using two landscape indices: the landscape disturbance index (LDI) and the landscape frangibility index (LFI). These indices evaluate both the internal vulnerability and external disturbance levels of ecosystems. The detailed formulas and descriptions are shown in Table 4.

The LDI quantifies the intensity of ecosystem impacts resulting from both natural and human factors. These indices are derived from a combination of three landscape metrics: the fragmentation index (Ci), the separation index (Si) and the dominance index (Di). According to previous studies (Liu *et al.* 2012; Gong *et al.* 2015; Ji *et al.* 2019), the weights for three landscape metrics were set at 0.5 (Ci), 0.3 (Si), and 0.2 (Di), respectively.

The LFI measures the resilience capacity of different landscape types in response to external disturbances. Based on the varying levels of resilience and sensitivity exhibited by these landscape types, a six-grade classification system was used to assess their fragility degree. Specifically, lower resistance corresponds to higher ecological risk, with urban areas considered the most stable and barren lands the most vulnerable (Liu *et al.* 2021; Du *et al.* 2023). Thus, the fragility degree was weighted as follows: urban (1), forest (2), grassland (3), cropland (4), water (5), and barren (6). The frangibility index of each landscape type was then normalized (Chen *et al.* 2020; Li *et al.* 2020; Wang *et al.* 2020).

The ERs represent the relative magnitude of comprehensive ecological losses within a given sampling unit, and they were calculated by combining LDI and LFI. A 25 km×25 km grid was used to obtain a total of 866 units through the fishnet construction tool in ArcGIS 10.6. The Kriging interpolation method was then employed to derive risk values and identify the geographical distribution of ERs in the URYR. Finally, the ERs were categorized into five grades using the Natural Breaks method: low risk, sub-low risk, medium risk, sub-high risk, and high risk.

Hot spot analysis We used the hot spot analysis tool and the Getis-Ord G_i^* local statistic in ArcGIS 10.6 to identify cold and hot spots for ESs and ERs. Whether a land unit was a hot or cold spot was determined by the aggregation index degree parameter Z (G_i^*). When Z (G_i^*)>0, the area was confirmed as having a denser cluster of hot spots; and *vice versa* (Getis and Ord 1992).

The specific formula is:

$$Z(G_i^*)=\frac{\sum_{j=1}^{n} w_{ij}x_j-\bar{x}\sum_{j=1}^{n} w_{ij}}{\sqrt{\frac{\left[n\sum_{j=1}^{n} w_{ij}^2-\left(\sum_{j=1}^{n} w_{ij}\right)^2\right]}{n-1}}} \quad (6)$$

where x_j is the ESs or ERs at cell j, $\bar{x}$ is the mean ESs or ERs, w_{ij} is the scale distance, and n is the number of the cells.

3. Results

3.1. Climate change

The projected future temperature trends show gradual increases across all three scenarios, with the highest growth rate observed under SSP5-8.5 (Fig. 3-B). Compared to temperature, the inter-annual variation of precipitation is more volatile across the three scenarios, generally following a pattern of initial increase, subsequent decrease, and eventual stabilization (Fig. 3-A).

Table 4 The calculation formulae for the landscape index

Landscape index	Formula	Formula description	Ecological meaning
Landscape fragmentation index	$C_i=n_i/A_i$	n_i is the patch number of landscape i; A_i is the total area of landscape i.	Describes the degree of patch fragmentation for a certain landscape type.
Landscape splitting index	$S_i=D_i\times A/A_i$, $D_i=(\frac{1}{2})\times\sqrt{n_i}/\sqrt{A}$	D_i is the patch density of landscape i; A is the total area of the entire landscape.	Indicates the degree of patch separation for a certain landscape type.
Landscape dominance index	$D_i=\frac{Q_i+M_i}{4}+L_i/2$, $Q_i=n_i/N_i$, $M_i=B_i/B$, $L_i=A_i/A$	N is the total number of patches; B_i is the sample number of patch i; B is the total number of samples.	Describes the degree of patch importance for a certain landscape type.
Landscape disturbance index	$LDI_i=aC_i+bS_i+cD_i$	a, b, and c are the weights of indices C_i, S_i, and D_i, respectively. $a+b+c=1$.	Quantifies the intensity of a landscape subjected to external interference.
Landscape disturbance index	–	According to the study area characteristics, we divided the fragility degree of the landscape types into five levels, then normalized them to obtain the individual vulnerability indexes.	Evaluates the internal capability to maintain stability for a certain landscape type.
Landscape ecological risk index	$LER=\sum_{i}^{N}\frac{S_{ki}}{S_k}\sqrt{LDI_i\times LFI_i}$	N is the number of landscape types in the sample areas; S is the area of landscape type i in sample k; S is the area of sample k.	Reflects the relative magnitudes of integrated ecological pressures caused by external interference and internal vulnerability for a certain study area.

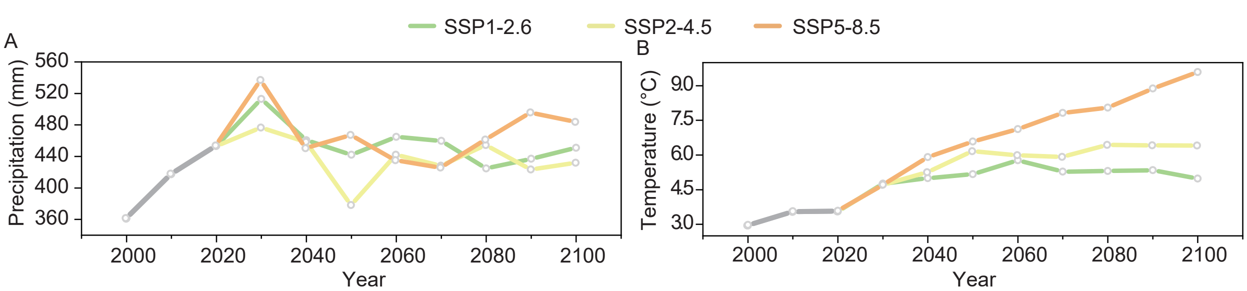

Fig. 3 Time series (2000–2100) of mean annual precipitation (A) and temperature (B) from the climate downscaling model under three scenarios across the upper reach of the Yellow River, China.

3.2. Land use change

The study area underwent significant changes in all land use types during 2000–2020. Notably, the largest proportion of grassland conversion involved 44,757 km^2, accounting for approximately 10% of the basin's total area. Specifically, 32,428 km^2 of grasslands were transferred to croplands, and 6,585 km^2 were turned into bare lands. Simultaneously, 46,707 km^2 of both bare lands and croplands were restored to grasslands. The conversion of other land types to urban land accounted for about 25% of the total urban area, although the proportion was relatively small (Fig. 4-R; Appendix C). Under SSP1-2.6, SSP2-4.5, and SSP5-8.5, other land types are projected to be converted into grasslands covering areas of 2,219, 6,361, and 2,359 km^2, respectively, which account for only a small proportion (Fig. 4-S–U; Appendices D–F).

3.3. Spatiotemporal dynamics of ecosystem services

The cross-validation indicated good predictive abilities of the models (Appendix G), with R^2 values of 0.56 (CS), 0.50 (SC), 0.66 (WY), and 0.64 (HQ). The correlations among the four ESs are significant ($P<0.001$).

The average CS in URYR increased from 6,235.85 to 6,269.95 Mg during 2000–2020 (Fig. 5-E). Higher CS was primarily distributed within the northern and western basin. During the historical period, high CS was observed in the Yellow River source area and grassland ecosystems in Qinghai Province. Compared to the historical period, upward trends in CS are projected in the future scenarios, particularly in regions such as Ordos, Baotou, and Bayannur located in the northern part of the URYR, except under SSP1-2.6 (Fig. 5-A and E).

The HQ improved from 0.84 to 0.85 over the past 20 years. Overall, high-value areas were predominantly

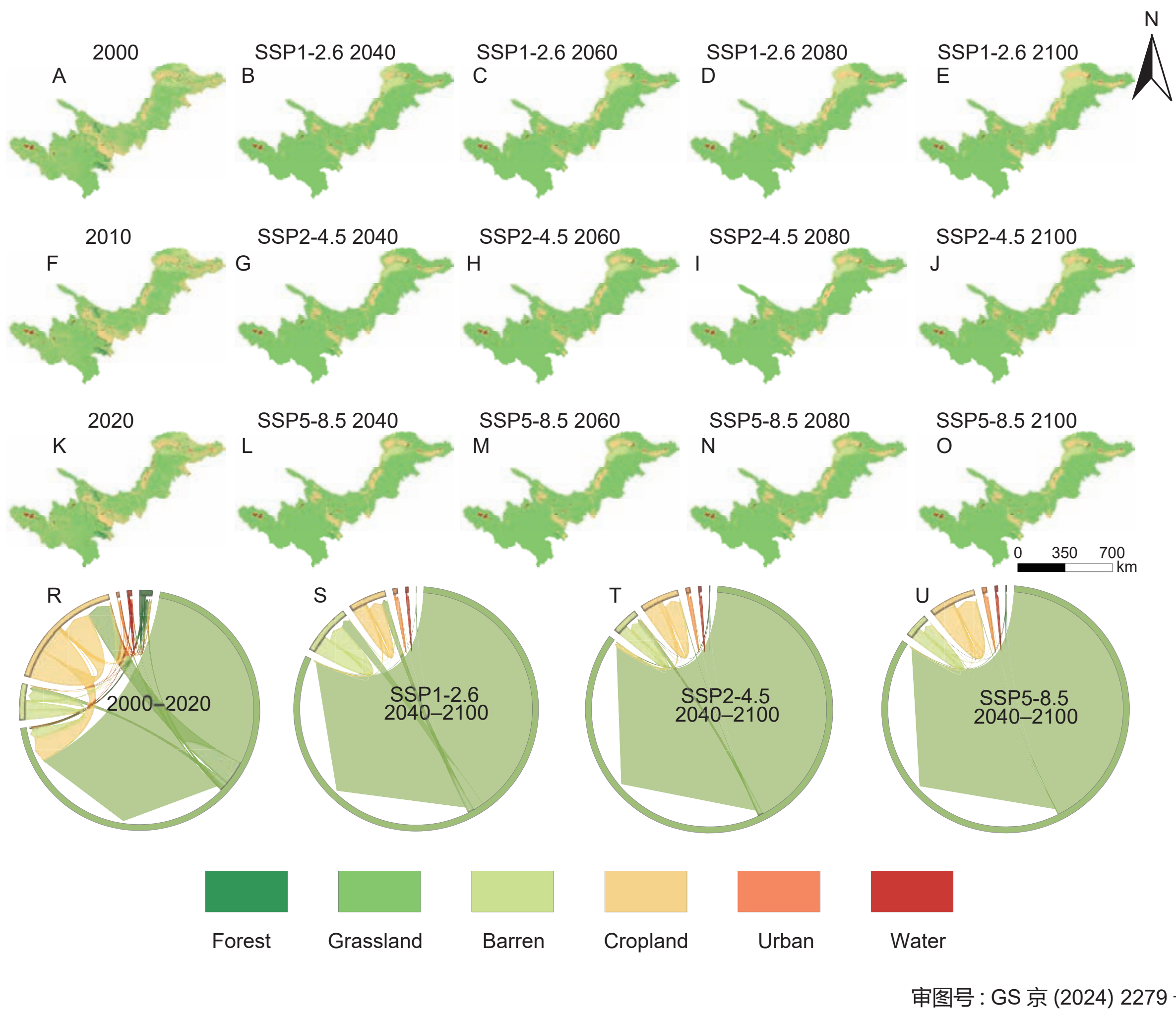

Fig. 4 Land use in the upper reach of the Yellow River, China. A–O, temporal and spatial changes of land use types. R–U, land use transfer matrices.

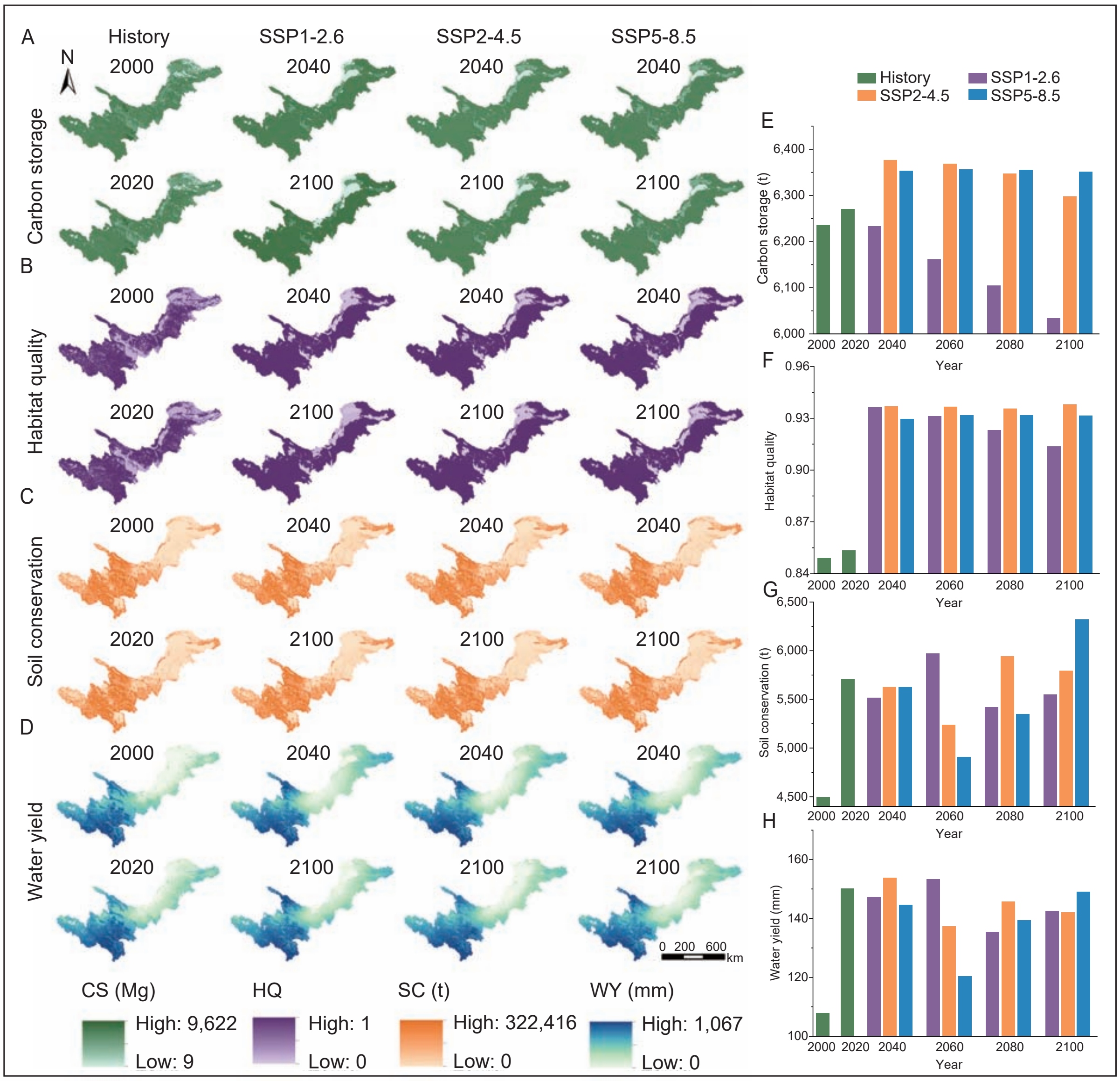

审图号：GS 京 (2024) 2279 号

Fig. 5 Ecosystem services in the upper reach of the Yellow River, China. A, temporal and spatial changes in carbon storage. B, temporal and spatial changes in habitat quality. C, temporal and spatial changes in soil conservation. D, temporal and spatial changes in water yield. E, carbon storage in different years. F, habitat quality in different years. G, soil conservation in different years. H, water yield in different years. CS, carbon storage; HQ, habitat quality; SC, soil conservation; WY, water yield.

distributed in the southwestern and central parts of the basin, while low HQ areas were primarily identified in Gansu Province and Inner Mongolia. The HQ is expected to improve under all three future scenarios, with high values distributed extensively across Qinghai Province and the Shaanxi section of the basin (Fig. 5-B and F).

The SC increased by approximately 1,200 t from 2000 to 2020. Higher levels of SC were predominantly found in Gansu and Qinghai provinces, whereas lower levels were found in Shaanxi and Inner Mongolia. Scenarios SSP2-4.5 and SSP5-8.5 demonstrate patterns with an initial decline followed by an increase in SC, with changes primarily occurring in the northeastern part of the URYR (Fig. 5-C and G).

From 2000 to 2020, the WY increased in the eastern region of Gansu Province. Spatially, high WY was primarily distributed in Qinghai Province and the eastern area of the URYR (Fig. 5-D). The WY is expected to be relatively low under the SSP5-8.5 scenario, while the other two scenarios exhibit trends with an initial decrease followed by a subsequent increase (Fig. 5-H).

3.4. Spatiotemporal dynamics of ecological risks

The distribution of ERs is generally lower in the western part of the URYR and higher in the eastern part under both historical and future scenarios (Fig. 6-A–O). There was an overall reduction in ERs in 2020 compared to 2000, particularly in the northern areas (e.g., Bayannur, Baotou, and Hohhot in Inner Mongolia), southwestern areas (e.g., Guoluo Tibetan Autonomous Prefecture and Huangnan Tibetan Autonomous Prefecture), and central areas (e.g., Lanzhou City and Baiyin City) (Fig. 6-A–C). Furthermore, sub-high risk and high-risk areas decreased by 27,673 km^2, equivalent to 6.23% of the total area (Fig. 6-R; Appendix H). In the future, ERs are projected to rise, with the areas of sub-high and high-risk zones increasing in northern Inner Mongolia. Meanwhile, areas of low, sub-low, and medium risk are expected to transition to sub-high and high risk under the SSP1-2.6, SSP2-4.5, and SSP5-8.5 scenarios, increasing by 13,273, 438, and 68 km^2, respectively. Nevertheless, ERs are projected to decline near Lanzhou City (Fig. 6-S–U; Appendices I–K).

3.5. Relationship between ESs and ERs

High-risk areas are primarily characterized by bare land. From 2000 to 2020, low-risk areas were mainly distributed in grasslands, water bodies, and forests, while medium-risk areas were located in croplands and urban areas (Fig. 7).

The spatial distributions of cold and hot spots for ESs and ERs are almost the opposite (Fig. 8). Generally, hot spots for ESs from 2000 to 2020 were found in the northeastern part of the URYR, while cold spots were in Qinghai Province, except for the Yushu Tibetan Autonomous Prefecture (Fig. 8-A–H). Conversely, hot spots for ERs were distributed in the northeast of the Inner Mongolia, while cold spots were located in southeastern Qinghai Province from 2000 to 2020 (Fig. 8-I and H). In the future scenarios, the hot spots of ERs are expected to be distributed in northern Ningxia and northern Shaanxi (Fig. 8-J–P). Furthermore, negative correlations between ESs and ERs are observed in both historical and future scenarios. Moreover, the

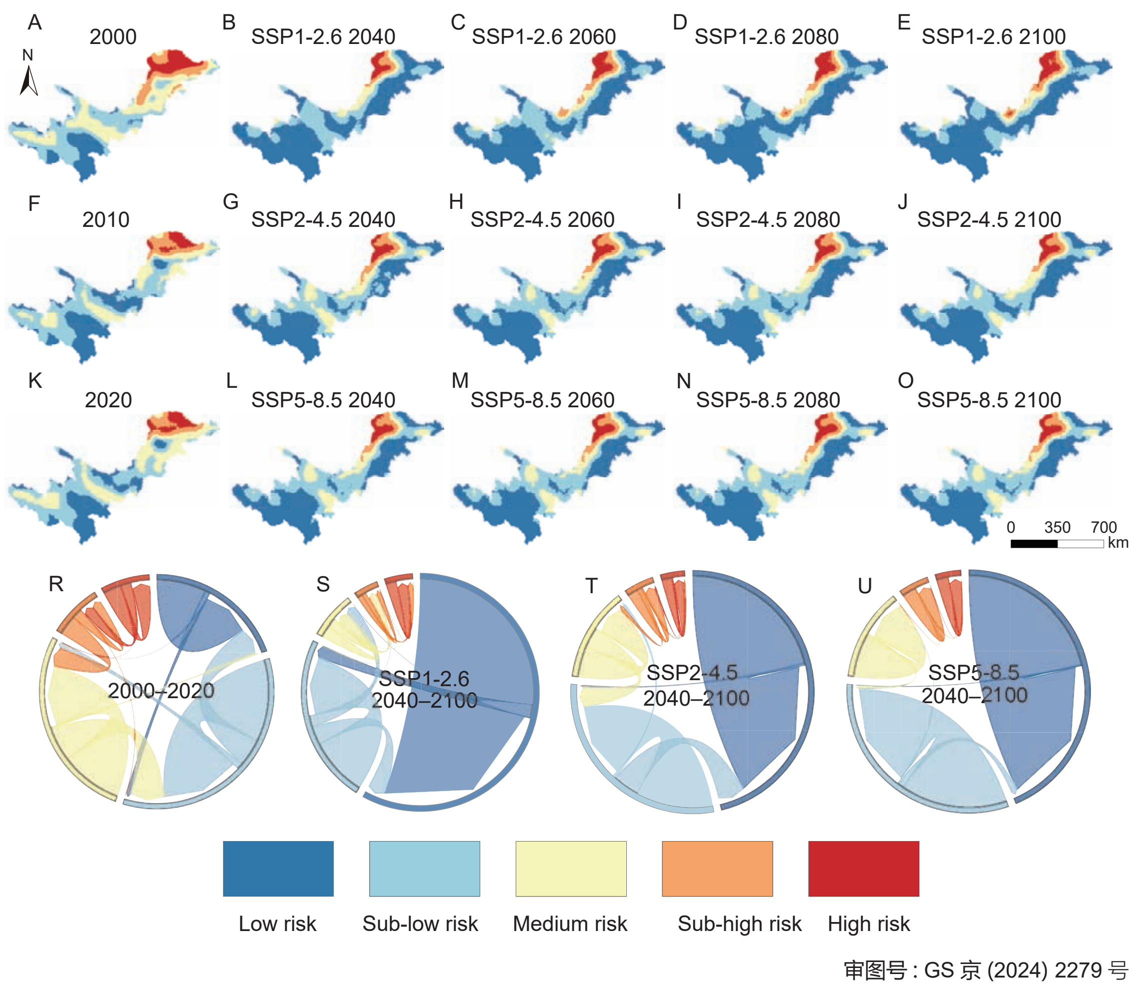

Fig. 6 Ecosystem risk in the upper reach of the Yellow River, China. A–O, temporal and spatial changes in ecosystem risk. R–U, ecosystem risk transfer matrices.

highest correlation coefficient is between CS and ERs, while SC shows the lowest correlation with the ERs.

The CS and ERs exhibit the strongest correlation under SSP1-2.6. Regarding the dynamics of HQ and ERs, their correlation coefficients are expected to be higher in future scenarios than in the past. Notably, there are negative relationships between SC and ERs under both SSP2-4.5 and SSP5-8.5. In the historical period, the correlation coefficients of WY with ERs were higher than in the future scenarios (Fig. 9).

4. Discussion

This study explored the ESs and ERs in the URYR, while considering the impacts of climate and land use changes. The main findings indicate that the source area of the URYR exhibits high ESs and low ERs, while the opposite is observed in the northeastern part of the basin. Regardless of the time or location, ESs consistently play a negative role in ERs. These insights are valuable for guiding future adaptation strategies under the principles of sustainable development in the Yellow River region.

4.1. Ecosystem services are negatively correlated with ecological risks

Temporally, the overall ERs in the URYR decreased from 2000 to 2020 (Fig. 6). This improvement can be attributed to the ecological construction efforts by the Chinese government. For instance, China invested $356.1 billion (1998–2015) in ecological projects such as Natural Forest Conservation Program and the Grain for Green Project (Bryan *et al.* 2018), which directly enhanced carbon sequestration (Wu *et al.* 2019). Additionally, YRCC (2020) reports that 252,400 km^2 of soil erosion had been controlled by the end of 2020. The soil and water conservation rate in the Yellow River Basin increased from 41.49% in 1990 to 66.94% in 2020, with average sediment discharge dropping to 240 million tons from 2001 to 2020

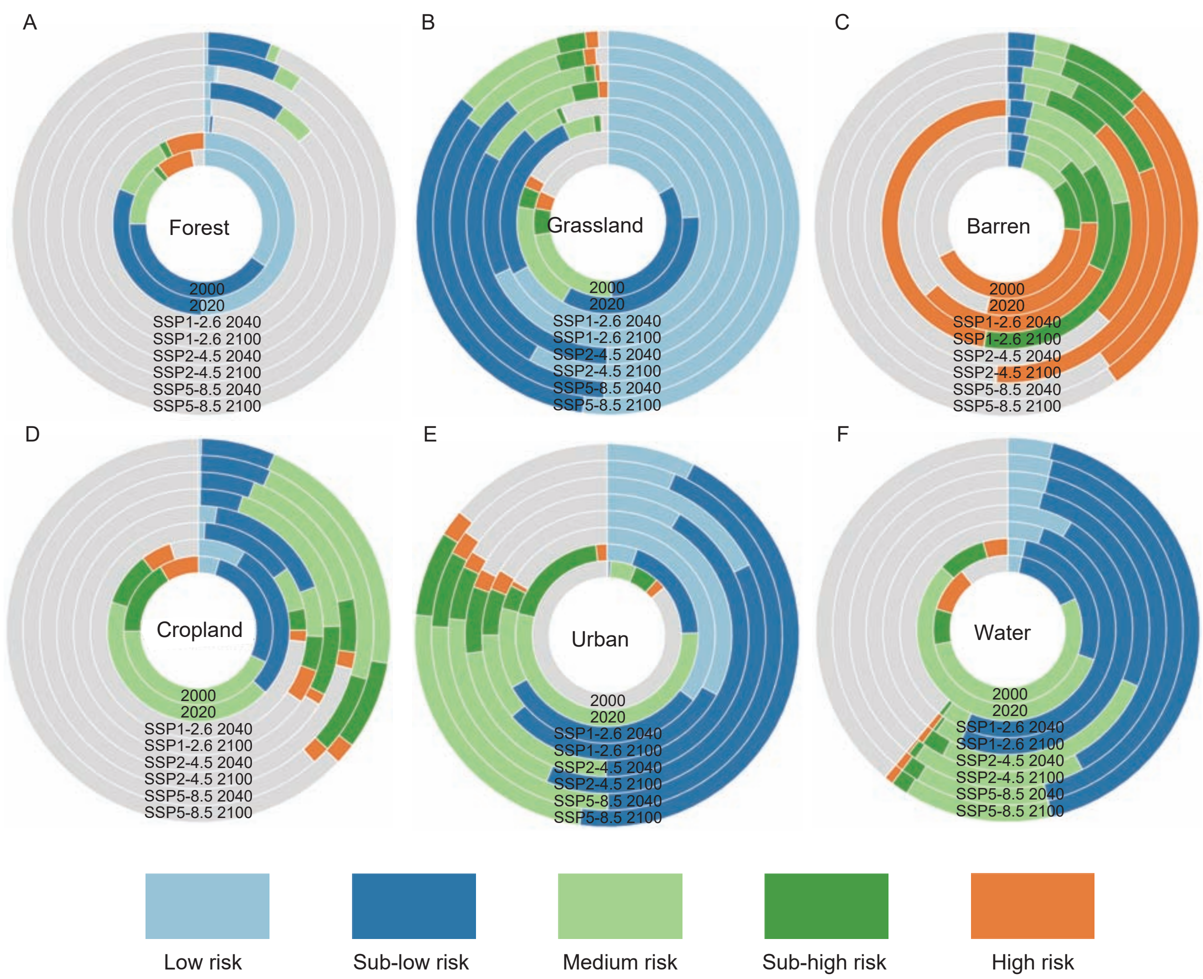

Fig. 7 Changes in area for different land use types as related to ecosystem risk categories.

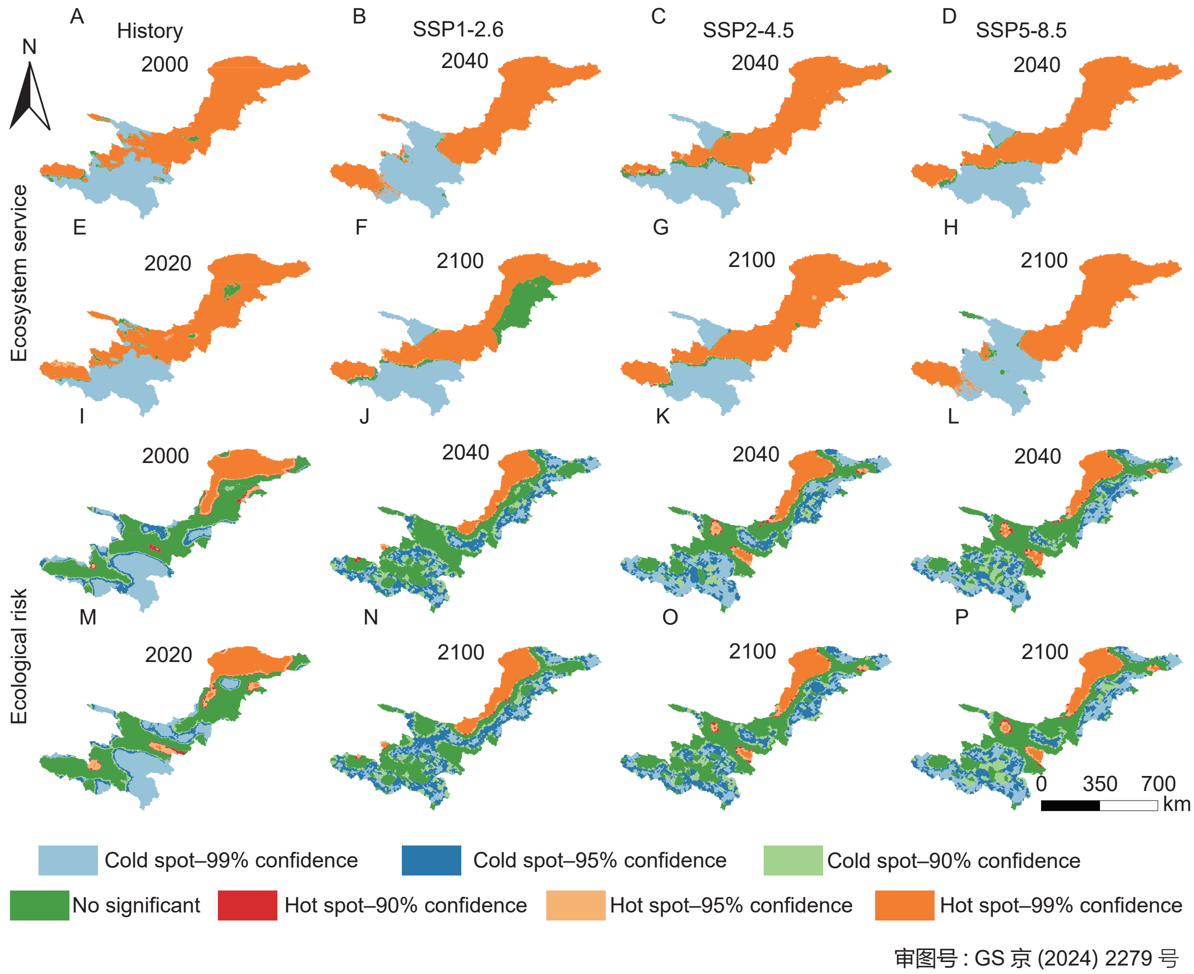

Fig. 8 Cold spots and hot spots of ecosystem services and ecosystem risks in the upper reach of the Yellow River, China.

(Wang *et al.* 2016). Despite these significant advances in ecological management, certain areas still face challenges such as a lack of vegetation diversity, ecological fragility, and unbalanced regional development. In addition, the absence of large-scale restoration projects in ecologically fragile areas of the Yellow River's source region during the late 20th century has resulted in slower ER mitigation (Qu *et al.* 2020; Zhang *et al.* 2020).

Spatially, ERs show significant heterogeneity under multiple pressures in the URYR. For example, in the Yushu and Guoluo Tibetan Autonomous Prefecture of Qinghai Province, where elevations exceed 4,000 m and alpine grasslands dominate, the ERs are generally lower due to the implementation of protection policies (Sun J *et al.* 2021a; Zhang *et al.* 2023). In the middle part of the URYR, around Lanzhou in Gansu Province, the ERs are moderate (Fig. 6). This can be attributed to favorable climatic conditions and minimal human interference, which contribute to plant growth (Song *et al.* 2018), wildlife survival, and the enhancement of grassland ESs (Zheng *et al.* 2022). However, in some areas, a dense population, and excessive industrial and agricultural activities exacerbate the ERs (Li B F *et al.* 2023). Additionally, urban expansion has increased the demands for external land and resources, leading to higher ERs and lower ESs in the northern part of the URYR. Therefore, promoting ESs is necessary to maintain ecosystem stability in this region (Zhang D H *et al.* 2022). In summary, a sustainable framework should be developed to strengthen ESs and reduce ERs in the future.

4.2. Ecological risks continue to increase under different scenarios

Under global change, the URYR faces severe challenges, including biodiversity decline and ecosystem degradation (Wohlfart *et al.* 2016; Zhang *et al.* 2018). Previous studies have shown that land use is closely correlated with ERs (Ju *et al.* 2021). In this study, all high-risk areas were situated in urban agglomerations, indicating that

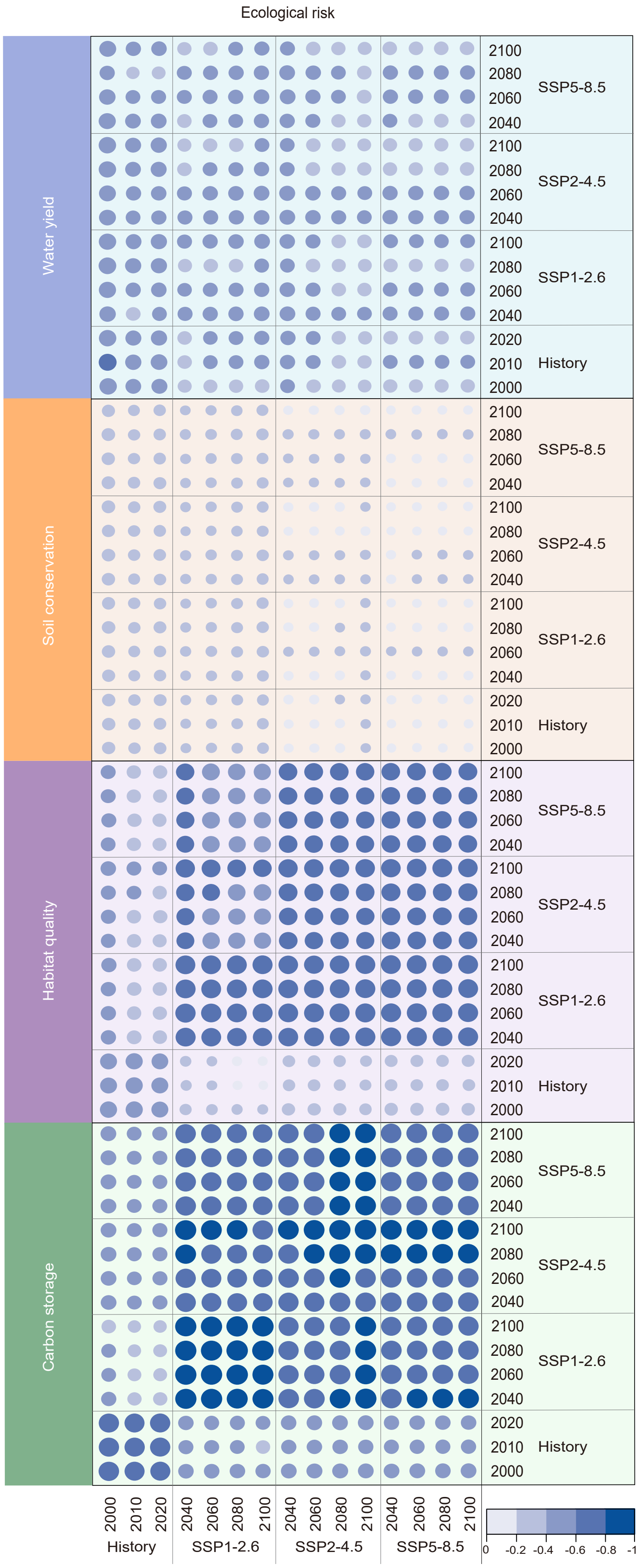

Fig. 9 Responses of ecosystem services and ecological risks.

urbanization leads to a decline in ESs and an increase in ERs, although the ERs rise at a faster rate than urbanization. Therefore, urban expansion and land fragmentation have become the main drivers of higher ERs (Tang *et al.* 2018; Gomes *et al.* 2020; Lin *et al.* 2021; Zhang S H *et al.* 2022). Conversely, the SSP5-8.5 scenario represents a development path driven by fossil fuels without ecological protection measures, leading to increasing ERs (Doelman *et al.* 2018). As a result, the low-risk and sub-low-risk areas in the URYR are more extensive under SSP1-2.6, due to the implementation of strict ecological protection policies (Gurney *et al.* 2022). Additionally, the simulation results under SSP2-4.5 demonstrate that unsustainable land use leads to continuous urban expansion, intensifying the competition with other land uses and increasing ERs (van Vliet *et al.* 2017; Zhang S H *et al.* 2022). In short, current land conservation and restoration management measures should primarily be informed by the SSP1-2.6 scenario to mitigate future climate and land use changes (Li H *et al.* 2022). Consequently, the Chinese government released the Master Plan for Major Projects of National Important Ecosystem Protection and Restoration (2021–2035) in 2020, which designated the Yellow River Basin as a key protection area (Zhang Q *et al.* 2022).

In summary, the future development of the URYR should focus on promoting an intensive, efficient, green, and low-carbon development path while implementing a differentiated regional coordinated development strategy (Guan *et al.* 2018) to mitigate the negative impacts of land use on ERs.

In this study, the Delta downscaling method and a multi-model ensemble were employed to improve the representativeness of the results, effectively addressing spatial vagueness and inconsistencies. Future research should consider additional policy and management factors, beyond just climate change and LUCC, to enhance the realism and relevance of the scenario simulations for regional policy formulation.

4.3. Adaptive management of the URYR according to ERs and ESs

Investigating the relationships among ERs, ESs, climate change, and land use can effectively integrate ecological dynamics into human well-being. As a key area of national ecological civilization construction, the Yellow River region has benefited greatly from large-scale ecological restoration measures such as the Three-North Forest Protection Project and the Grain for Green Project, which have significantly improved vegetation coverage and ESs (Guo *et al.* 2022). Moreover, China has announced the ecological protection and high-quality development of the Yellow River Basin as a national strategy (Lu and Sun 2019), which places higher demands on ecological protection in the URYR. Under these circumstances, our findings are pivotal for watershed protection and the sustainable development of ecosystems. According to the distribution patterns of ESs and ERs, we divided the study area into four regions to ensure regional ecological security (Liu *et al.* 2012) (Fig. 10).

First, the high ER–low ES area is primarily distributed in the northeastern part of the URYR, including Bayannur, Baotou, Hohhot City, and parts of Inner Mongolia. In this area, effective environmental protection measures should be implemented to improve ecosystem functions and services in the future. From the natural perspective, regional landscape stability should be maintained to enhance ecosystem resistance to external threats. Additionally, more ecological protection areas should be established to prevent over-exploitation and human interference. Strengthening education, multifaceted management, and energy structure adjustments are also recommended to promote ecological civilization (Dou *et al.* 2020; Sun *et al.* 2022).

Second, the high ER–high ES area, located in the middle part of the URYR (including Haidong district of Qinghai Province, Lanzhou, Baiyin, and Wuwei), is a key hydropower base due to its abundant water resources. However, potential ERs might increase with the development and construction of hydropower stations. To address the current ERs, the government should optimize land use patterns and reduce human intervention and over-exploitation to ensure ecosystem health (Yang *et al.* 2019; Wang *et al.* 2023). Therefore, regional management should balance ecological protection with sustainable development (Guan *et al.* 2018).

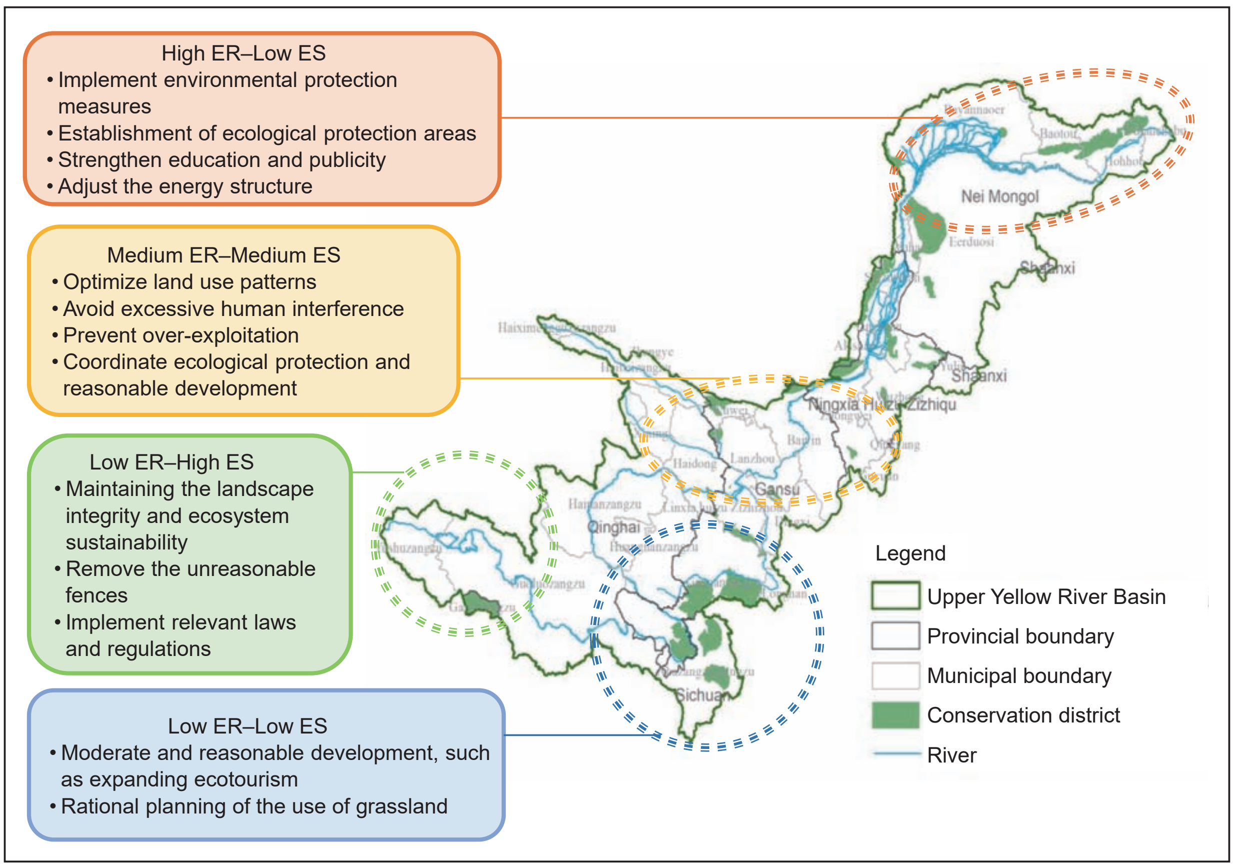

审图号 : GS 京 (2024) 2279 号

Fig. 10 Adaptive management of the upper reach of the Yellow River, China. ER, ecosystem risk; ES, ecosystem service.

Third, the low ER–low ES area includes Aba Tibetan Autonomous Prefecture, Gannan Tibetan Autonomous Prefecture, and Huangnan Tibetan Autonomous Prefecture. In these regions, the ERs are effectively balanced with the ESs, making moderate development feasible, such as ecotourism (Liu *et al.* 2023). In addition, grassland utilization should consider its health status and local socio-economic characteristics to achieve sustainable development (Li R W *et al.* 2023).

Finally, the low ER–high ES area, located in Yushu Tibetan Autonomous Prefecture and some grassland areas in Qinghai Province, is relatively robust and resistant to climate change and human activities. Recently, a series of major ecological projects have been implemented in this region, which have remarkably improved the ESs and reduced the ERs (Li R W *et al.* 2023). Meanwhile, reasonable grazing practices promote the ecosystem energy cycle, improve ecosystem functioning, and consequently increase the herdsmen's incomes (Sun *et al.* 2020). In the next phase, we call for maintaining landscape integrity and ecosystem sustainability (Sun *et al.* 2022), removing unnecessary fences from healthy grassland ecosystems (Sun *et al.* 2020; Sun J *et al.* 2021b), focusing on Goal 15 (life on land) of the Sustainable Development Goals, and rigorously implementing the *Tibetan Plateau Ecological Protection Law of the People's Republic of China* (Sun J *et al.* 2021a).

5. Conclusion

This study addresses the research gap concerning the complex spatial interactions between different ESs and ERs during historical and future periods in the URYR. The results reveal significant spatial heterogeneity in the ESs and ERs due to considerable differences in elevation, climatic elements, land use types and management practices. Specifically, areas of high ESs and low ERs are mainly distributed in the source area of the Yellow River, while areas of low ESs and high ERs are concentrated on the northeast of the URYR, and they are regulated by grassland ecosystem functions and urbanization, respectively. In the long term, ER areas are expected to gradually decrease while ESs will be enhanced through the protection of ecological projects, nature reserves, and national parks. Nevertheless, attention must be paid to the potential increases in the ER area under the three different future scenarios, and they are closely related to climate change and land use. In conclusion, we propose a framework for optimizing the regional spatial layout to protect and develop the URYR in the future.

Acknowledgements

This research was supported by the Ecological Conservation and High-Quality Development of the Yellow River Basin Program, China (2022-YRUC-01-0102), the Second Tibetan Plateau Scientific Expedition and Research Program, China (20190ZKK0405), and the Basic Research Fund Project of Innovation Team of Novel Forage Germplasm and Sustainable Utilization of Grassland Resources, China (BR22-12-07).

Declaration of competing interests

The authors declare that they have no conflict of interest.

Appendices associated with this paper are available at https://doi.org/10.1016/j.jia.2024.09.015

References

Ali M A, Bilal M, Wang Y, Qiu Z F, Nichol J E, de Leeuw G, Ke S, Mhawish A, Almazroui M, Mazhar U, Habtemicheal B A, Islam M N. 2022. Evaluation and comparison of CMIP6 models and MERRA-2 reanalysis AOD against Satellite observations from 2000 to 2014 over China. *Geoscience Frontiers*, **13**, 101325.

Aneseyee A B, Soromessa T, Elias E, Noszczyk T, Feyisa G L. 2022. Evaluation of water provision ecosystem services associated with land use/cover and climate variability in the winike watershed, Omo Gibe Basin of Ethiopia. *Environmental Management*, **69**, 367–383.

Bennett E M. 2017. Research frontiers in ecosystem service science. *Ecosystems*, **20**, 31–37.

Best J. 2019. Anthropogenic stresses on the world's big rivers. *Nature Geoscience*, **12**, 7–21.

Bryan B A, Gao L, Ye Y Q, Sun X F, Connor J D, Crossman N D, Stafford-Smith M, Wu J G, He C Y, Yu D Y, Liu Z F, Li A, Huang Q X, Ren H, Deng X Z, Zheng H, Niu J M, Han G D, Hou X Y. 2018. China's response to a national land-system sustainability emergency. *Nature*, **559**, 193–204.

Cai G, Xiong J F, Wen L S, Weng A F, Lin Y Y, Li B Y. 2023. Predicting the ecosystem service values and constructing ecological security patterns in future changing land use patterns. *Ecological Indicators*, **154**, 110787.

Cao Q, Zhang X W, Lei D M, Guo L Y, Sun X H, Kong F E, Wu J S. 2019. Multi-scenario simulation of landscape ecological risk probability to facilitate different decision-making preferences. *Journal of Cleaner Production*, **227**, 325–335.

Chen D S, Jiang P H, Li M C. 2021. Assessing potential ecosystem service dynamics driven by urbanization in the Yangtze River Economic Belt, China. *Journal of Environmental Management*, **292**, 112734.

Chen F H, Fu B J, Xia J, Wu D, Wu S H, Zhang Y L, Sun H, Liu Y, Fang X M, Qin B Q, Li X, Zhang T J, Liu B Y, Dong Z B, Hou S G, Tian L D, Xu B Q, Dong G H, Zheng J Y, Yang W, *et al.* 2019. Major advances in studies of the physical geography and living environment of China during the past 70 years and future prospects. *Science China* (Earth Sciences), **62**, 1665–1701.

Chen J, Dong B, Li H R, Zhang S S, Peng L, Fang L, Zhang C B, Li S. 2020. Study on landscape ecological risk assessment of Hooded Crane breeding and overwintering habitat. *Environmental Research*, **187**, 109649.

Chen W X, Zeng J, Zhong M X, Pan S P. 2021. Coupling analysis of ecosystem services value and economic development in the Yangtze River economic belt: A case study in Hunan Province, China. *Remote Sensing*, **13**, 1552.

Costanza R, d'Arge R, de Groot R, Farber S, Grasso M, Hannon B, Limburg K, Naeem S, O'Neill R V, Paruelo J, Raskin R G, Sutton P, van den Belt M. 1997. The value of the world's ecosystem services and natural capital. *Nature*, **387**, 253–260.

Doelman J C, Stehfest E, Tabeau A, van Meijl H, Lassaletta L, Gernaat D, Hermans K, Harmsen M, Daioglou V, Biemans H, van der Sluis S, van Vuuren D P. 2018. Exploring SSP land-use dynamics using the IMAGE model: Regional and gridded scenarios of land-use change and land-based climate change mitigation. *Global Environmental Change* (Human and Policy Dimensions), **48**, 119–135.

Dou H S, Li X B, Li S K, Dang D L, Li X, Lyu X, Li M Y, Liu S Y. 2020. Mapping ecosystem services bundles for analyzing spatial trade-offs in Inner Mongolia, China. *Journal of Cleaner Production*, **256**, 120444.

Du L D, Dong C, Kang X C, Qian X L, Gu L X. 2023. Spatiotemporal evolution of land cover changes and landscape ecological risk assessment in the Yellow River Basin, 2015–2020. *Journal of Environmental Management*, **332**, 117149.

Fan J, Wang Y F, Wang Y X. 2020. High quality regional development research based on geographical units: Discuss on the difference in development conditions and priorities of the Yellow River Basin compared to the Yangtze River Basin. *Economic Geography*, **40**, 1–11. (in Chinese)

Gao L N, Tao F, Liu R R, Wang Z L, Leng H J, Zhou T. 2022. Multi-scenario simulation and ecological risk analysis of land use based on the PLUS model: A case study of Nanjing. *Sustainable Cities and Society*, **85**, 104055.

Getis A, Ord J K. 1992. The analysis of spatial association by use of distance statistics. *Geographical Analysis*, **24**, 189–206.

Gomes L C, Bianchi F J J A, Cardoso I M, Schulte R P O, Arts B J M, Fernandes Filho E I. 2020. Land use and land cover scenarios: An interdisciplinary approach integrating local conditions and the global shared socioeconomic pathways. *Land Use Policy*, **97**, 104723.

Gong J, Yang J X, Tang W W. 2015. Spatially explicit landscape-level ecological risks induced by land use and land cover change in a national ecologically representative region in China. *International Journal of Environmental Research and Public Health*, **12**, 14192–14215.

Guan X L, Wei H K, Lu S S, Dai Q, Su H J. 2018. Assessment on the urbanization strategy in China: Achievements, challenges and reflections. *Habitat International*, **71**, 97–109.

Guo S S, Wu C Y, Wang Y H, Qiu G Q, Zhu D, Niu Q, Qin L. 2022. Threshold effect of ecosystem services in response to climate change, human activity and landscape pattern in the upper and middle Yellow River of China. *Ecological Indicators*, **136**, 108603.

Gurney K R, Kilkis S, Seto K C, Lwasa S, Moran D, Riahi K, Keller M, Rayner P, Luqman M. 2022. Greenhouse gas emissions from global cities under SSP/RCP scenarios, 1990 to 2100. *Global Environmental Change* (Human and Policy Dimensions), **73**, 102478.

Hou Y, Lü Y H, Chen W P, Fu B J. 2017. Temporal variation and spatial scale dependency of ecosystem service interactions: A case study on the central Loess Plateau of China. *Landscape Ecology*, **32**, 1201–1217.

Huang H, Xue J, Feng X, Zhao J, Sun H, Hu Y, Ma Y. 2024. Thriving arid oasis urban agglomerations: Optimizing ecosystem services pattern under future climate change scenarios using dynamic Bayesian network. *Journal of Environmental Management*, **350**, 119612.

Huang S W, Song W, Gao H, Cao C J, Li J F, Liu B, Yu H, Li S C, Wei X, Sheng S Q. 2023. Association between ecological risks and ecosystem services in an urban agglomeration in arid China. *Frontiers in Environmental Science*, **10**, 2022.

Islam M, Yamaguchi R, Sugiawan Y, Managi S. 2019. Valuing natural capital and ecosystem services: A literature review. *Sustainability Science*, **14**, 159–174.

Ji X, Jin Y X, Mao X F. 2019. Ecological risk assessment of cities on the Tibetan Plateau based on land use/land cover changes — Case study of Delingha City. *Ecological Indicators*, **101**, 185–191.

Jiang L, O'Neill B C. 2017. Global urbanization projections for the shared socioeconomic pathways. *Global Environmental Change*, **42**, 193–199.

Jiang Z, Gan X Y, Liu J, Bi X, Kang A, Zhou B. 2023. Landscape ecological risk assessment and zoning control based on ecosystem service value: Taking Sichuan Province as an example. *Applied Sciences*, **13**, 12103.

Ju H R, Niu C Y, Zhang S R, Jiang W, Zhang Z H, Zhang X L, Yang Z Y, Cui Y R. 2021. Spatiotemporal patterns and modifiable areal unit problems of the landscape ecological risk in coastal areas: A case study of the Shandong Peninsula, China. *Journal of Cleaner Production*, **310**, 127522.

Li B F, Feng Q, Wang X, Li Z J, Wang F, Zhao C G, Yu T F, Chen W Y. 2023. Formation of the upper reaches of the Yellow River: Provenance evidence from the strata of the Yellow River sedimentary basin. *Global and Planetary Change*, **229**, 104224.

Li C, Raj Kattel G, Zhang J, Shang Y, Gnyawali K R, Zhang F, Miao L J. 2022. Slightly enhanced drought in the Yellow River Basin under future warming scenarios. *Atmospheric Research*, **280**, 106423.

Li C H, Wei Y F, Liu Y F, Li L L, Peng L X, Chen J X, Liu L H, Dou T B, Wu X D. 2022. Active layer thickness in the Northern Hemisphere: Changes From 2000 to 2018 and future simulations. *Journal of Geophysical Research* (Atmospheres), **127**, e2022JD036785.

Li C W, Fang S B, Geng X L, Yuan Y, Zheng X W, Zhang D, Li R X, Sun W, Wang X R. 2023. Coastal ecosystem service in response to past and future land use and land cover change dynamics in the Yangtze river estuary. *Journal of Cleaner Production*, **385**, 135601.

Li J H, Gao M X. 2019. Spatiotemporal evolution and correlation analysis of ecosystem service values and ecological risk in Binzhou. *Acta Ecologica Sinica*, **39**, 7815–7827. (in Chinese)

Li R W, Han G D, Sun J, Zhou T C, Chen J H, He W, Wang Y. 2023. Dynamics and controls of ecosystem multiserviceability across the Qingzang Plateau. *Geography and Sustainability*, **4**, 318–328.

Li W J, Wang Y, Xie S Y, Sun R H, Cheng X. 2020. Impacts of landscape multifunctionality change on landscape ecological risk in a megacity, China: A case study of Beijing. *Ecological Indicators*, **117**, 106681.

Lin J H, Lin M S, Chen W H, Zhang A, Qi X H, Hou H R. 2021. Ecological risks of geological disasters and the patterns of the urban agglomeration in the Fujian Delta region. *Ecological Indicators*, **125**, 107475.

Lin Y Y, Hu X S, Zheng X X, Hou X Y, Zhang Z X, Zhou X N, Qiu R Z, Lin J G. 2019. Spatial variations in the relationships between road network and landscape ecological risks in the highest forest coverage region of China. *Ecological Indicators*, **96**, 392–403.

Liu D D, Qu R J, Zhao C H, Liu A P, Deng X Z. 2012. Landscape ecological risk assessment in Yellow River Delta. *Journal of Food Agriculture & Environment*, **10**, 970–972.

Liu F L, Yang L, Wang S. 2023. Spatial and temporal evolution and correlation analysis of landscape ecological risks and ecosystem service values in the Jinsha River Basin. *Journal of Resources and Ecology*, **14**, 914–927. (in Chinese)

Liu L, Cao W, Shao Q Q, Huang L, He T. 2016. Characteristics of land use/cover and macroscopic ecological changes in the headwaters of the yangtze river and of the Yellow River over the past 30 years. *Sustainability*, **8**, 237.

Liu X Z, Li X S, Jiang D M. 2021. Landscape pattern identification and ecological risk assessment using land-use change in the Yellow River Basin. *Transactions of the Chinese Society of Agricultural Engineering*, **37**, 265–274. (in Chinese)

Liu Y X, Peng J, Zhang T, Zhao M Y. 2016. Assessing landscape eco-risk associated with hilly construction land exploitation in the southwest of China: Trade-off and adaptation. *Ecological Indicators*, **62**, 289–297.

Lu D D, Sun D Q. 2019. Development and management tasks of the Yellow River Basin: A preliminary understanding and suggestion. *Acta Geographica Sinica*, **74**, 2431–2436. (in Chinese)

Lu K D, Arshad M, Ma X Y, Ullah I, Wang J J, Shao W. 2022. Evaluating observed and future spatiotemporal changes in precipitation and temperature across China based on CMIP6-GCMs. *International Journal of Climatology*, **42**, 7703–7729.

Lufafa A, Tenywa M M, Isabirye M, Majaliwa M J G, Woomer P L. 2003. Prediction of soil erosion in a Lake Victoria basin catchment using a GIS-based Universal Soil Loss model. *Agricultural Systems*, **76**, 883–894.

Maes M J A, Jones K E, Toledano M B, Milligan B. 2019. Mapping synergies and trade-offs between urban ecosystems and the sustainable development goals. *Environmental Science & Policy*, **93**, 181–188.

Magalhães Filho L N L, Roebeling P C, Costa L F C, de Lima L T. 2022. Ecosystem services values at risk in the Atlantic coastal zone due to sea-level rise and socioeconomic development. *Ecosystem Services*, **58**, 101492.

Mann D, Anees M M, Rankavat S, Joshi P K. 2021. Spatio-temporal variations in landscape ecological risk related to road network in the Central Himalaya. *Human and Ecological Risk Assessment*, **27**, 289–306.

Mo W B, Wang Y, Zhang Y X, Zhuang D F. 2017. Impacts of road network expansion on landscape ecological risk in a megacity, China: A case study of Beijing. *Science of the Total Environment*, **574**, 1000–1011.

Moreno A, Hasenauer H. 2016. Spatial downscaling of European climate data. *International Journal of Climatology*, **36**, 1444–1458.

Peng S Z, Gang C C, Cao Y, Chen Y. 2018. Assessment of climate change trends over the Loess Plateau in China from 1901 to 2100. *International Journal of Climatology*, **38**, 2250–2264.

Qi Z X, Cai Y P, Lin J Y, Xie Y L, Yao L L, Zhang P, Wang Y Y, Guo H J. 2023. Coupled high-resolution GCM downscaling framework for projecting dynamics and drivers of ecosystem services in Pearl River Basin, China. *Ecological Indicators*, **154**, 110770.

Qi Z X, Sun L, Cai Y P, Xie Y L, Yao L L, Li B W, Ye Y C. 2024. Spatial-temporal dynamics of population exposure to compound extreme heat-precipitation events under multiple scenarios for Pearl River Basin, China. *Climate Services*, **34**, 100477.

Qin J S, Buda S U, Tao H, Wang Y J, Huang J L, Jiang T. 2021. Projection of temperature and precipitation under SSPs-RCPs Scenarios over northwest China. *Frontiers in Earth Science*, **15**, 15.

Qu S J, Hu S G, Li W D, Wang H, Zhang C R, Li Q F. 2020. Interaction between urban land expansion and land use policy: An analysis using the DPSIR framework. *Land Use Policy*, **99**, 4856.

Song J, Wan S Q, Peng S S, Piao S L, Ciais P, Han X G, Zeng D H, Cao G M, Wang Q B, Bai W M, Liu L L. 2018. The carbon sequestration potential of China's grasslands. *Ecosphere*, **9**, e02452.

Song J B, Zhang Q, Wu W H, Singh V, Shen Z X, Wang G, Xu C Y. 2022. Amplifying flood risk across the Lower Yellow River Basin, China, under shared socioeconomic pathways. *Frontiers in Earth Science*, **10**, 900866.

Su B D, Huang J L, Mondal S K, Zhai J Q, Wang Y J, Wen S S, Gao M N, Lv Y R, Jiang S, Jiang T, Li A W. 2021. Insight from CMIP6 SSP-RCP scenarios for future drought characteristics in China. *Atmospheric Research*, **250**, 105375.

Sun J, Fu B J, Zhao W W, Liu S L, Liu G H, Zhou H K, Shao X Q, Chen Y C, Zhang Y, Deng Y F. 2021a. Optimizing grazing exclusion practices to achieve Goal 15 of the sustainable development goals in the Tibetan Plateau. *Science Bulletin*, **66**, 1493–1496.

Sun J, Liang E Y, Barrio I C, Chen J, Wang J N, Fu B J. 2021b. Fences undermine biodiversity targets. *Science*, **374**, 269.

Sun J, Liu M, Fu B J, Kemp D, Zhao W W, Liu G H, Han G D, Wilkes A, Lu X Y, Chen Y C, Cheng G W, Zhou T C, Hou G, Zhan T Y, Peng F, Shang H, Xu M, Shi P L, He Y T, Li M, *et al.* 2020. Reconsidering the efficiency of grazing exclusion using fences on the Tibetan Plateau. *Science Bulletin*, **65**, 1405–1414.

Sun J, Wang Y, Piao S L, Liu M, Han G D, Li J R, Liang E Y, Lee T M, Liu G H, Wilkes A, Liu S L, Zhao W W, Zhou H K, Yibeltal M, Berihun M L, Browning D, Fenta A A, Tsunekawa A, Brown J, Willms W, *et al.* 2022. Toward a sustainable grassland ecosystem worldwide. *Innovation*, **3**, 100265.

Sun M H, Niu W H, Zhang B B, Geng Q L, Yu Q. 2021. Spatial-temporal evolution and responses of ecosystem service value under land use change in the Yellow River Basin: A case study of Shaanxi-Gansu-Ningxia region, Northwest China. *Chinese Journal of Applied Ecology*, **32**, 3913–3922. (in Chinese)

Sun S, Dai T L, Wang Z Y, Chou J M, Chao Q C, Shi P J. 2021. Projected increases in population exposure of daily climate extremes in eastern China by 2050. *Advances in Climate Change Research*, **12**, 804–813.

Sun S, Shi Q. 2020. Global spatio-temporal assessment of changes in multiple ecosystem services under four IPCC SRES land-use scenarios. *Earth's Future*, **8**, e2020EF001668.

Tang L N, Wang L, Li Q Y, Zhao J Z. 2018. A framework designation for the assessment of urban ecological risks. *International Journal of Sustainable Development and World Ecology*, **25**, 387–395.

van Vliet J, Eitelberg D A, Verburg P H. 2017. A global analysis of land take in cropland areas and production displacement from urbanization. *Global Environmental Change*, **43**, 107–115.

Wang B B, Ding M J, Li S C, Liu L S, Ai J H. 2020. Assessment of landscape ecological risk for a cross-border basin: A case study of the Koshi River Basin, central Himalayas. *Ecological Indicators*, **117**, 106621.

Wang H, Liu X M, Zhao C Y, Chang Y P, Liu Y Y, Zang F. 2021. Spatial-temporal pattern analysis of landscape ecological risk assessment based on land use/land cover change in Baishuijiang National nature reserve in Gansu Province, China. *Ecological Indicators*, **124**, 107454.

Wang S, Fu B J, Piao S L, Lü Y H, Ciais P, Feng X M, Wang Y F. 2016. Reduced sediment transport in the Yellow River due to anthropogenic changes. *Nature Geoscience*, **9**, 38–41.

Wang T, Li H B, Huang Y. 2021. The complex ecological network's resilience of the Wuhan metropolitan area. *Ecological Indicators*, **130**, 108101.

Wang Y, Chen Y P, Wang H J, Lv Y H, Hao Y B, Cui X Y, Wang Y Z, Hu R H, Xue K, Fu B J. 2021. Ecosystem change and its ecohydrological effect in the Yellow River Basin. *Bulletin of National Natural Science Foundation of China*, **35**, 520–528. (in Chinese)

Wang Y S, Yang Z H, Yu M H, Lin R Y, Zhu L, Bai F P. 2023. Integrating ecosystem health and services for assessing ecological risk and its response to typical land-use patterns in the eco-fragile region, North China. *Environmental Management*, **71**, 867–884.

Wohlfart C, Kuenzer C, Chen C, Liu G H. 2016. Social-ecological challenges in the Yellow River basin (China): A review. *Environmental Earth Sciences*, **75**, 1066.

Wu X T, Wang S, Fu B J, Feng X M, Chen Y Z. 2019. Socio-ecological changes on the Loess Plateau of China after grain to green program. *Science of the Total Environment*, **678**, 565–573.

Xing L, Hu M S, Wang Y. 2020. Integrating ecosystem services value and uncertainty into regional ecological risk assessment: A case study of Hubei Province, Central China. *Science of the Total Environment*, **740**, 140126.

Yang Y J, Song G, Lu S. 2020. Assessment of land ecosystem health with Monte Carlo simulation: A case study in Qiqihaer, China. *Journal of Cleaner Production*, **250**, 119522.

Yang Y Y, Zheng H, Kong L Q, Huang B B, Xu W H, Ouyang Z Y. 2019. Mapping ecosystem services bundles to detect high- and low-value ecosystem services areas for land use management. *Journal of Cleaner Production*, **225**, 11–17.

YRCC (Yellow River Conservancy Commission). 2020. Soil and Water Conservation Bulletin of the Yellow River Basin. [2020-11-10]. http://www.yrcc.gov.cn/ (in Chinese)

Zhai J Q, Mondal S K, Fischer T, Wang Y J, Su B D, Huang J L, Tao H, Wang G J, Ullah W, Uddin M J. 2020. Future drought characteristics through a multi-model ensemble from CMIP6 over South Asia. *Atmospheric Research*, **246**, 105111.

Zhang D H, Jing P Q, Sun P J, Ren H H, Ai Z M. 2022. The non-significant correlation between landscape ecological risk and ecosystem services in Xi'an Metropolitan Area, China. *Ecological Indicators*, **141**, 109118.

Zhang K L, Fang B, Zhang Z C, Liu T, Liu K. 2024. Exploring future ecosystem service changes and key contributing factors from a "past-future-action" perspective: A case study of the Yellow River Basin. *Science of The Total Environment*, **926**, 171630.

Zhang Q, Wang G, Yuan R Y, Singh V P, Wu W H, Wang D Z. 2022. Dynamic responses of ecological vulnerability to land cover shifts over the Yellow river Basin, China. *Ecological Indicators*, **144**, 109554.

Zhang Q, Zhang Z J, Shi P J, Singh V P, Gu X H. 2018. Evaluation of ecological instream flow considering hydrological alterations in the Yellow River basin, China. *Global and Planetary Change*, **160**, 61–74.

Zhang S D, Wu T, Guo L, Zhao Y L. 2023. Assessing ecological risk on the Qinghai-Tibet Plateau based on future land use scenarios and ecosystem service values. *Ecological Indicators*, **154**, 110769.

Zhang S H, Zhong Q L, Cheng D L, Xu C B, Chang Y N, Lin Y Y, Li B Y. 2022. Landscape ecological risk projection based on the PLUS model under the localized shared socioeconomic pathways in the Fujian Delta region. *Ecological Indicators*, **136**, 108642.

Zhang W, Chang W J, Zhu Z C, Hui Z. 2020. Landscape ecological risk assessment of Chinese coastal cities based on land use change. *Applied Geography*, **117**, 2174.

Zheng H Y, Miao C Y, Li X Y, Kong D X, Gou J J, Wu J W, Zhang S P. 2022. Effects of vegetation changes and multiple environmental factors on evapotranspiration across China over the past 34 years. *Earths Future*, **10**, e2021EF002564.

Zhou Z X, Robinson G M, Song B J. 2019. Experimental research on trade-offs in ecosystem services: The agro-ecosystem functional spectrum. *Ecological Indicators*, **106**, 105536.

Zhu X, Lee S Y, Wen X H, Ji Z M, Lin L, Wei Z G, Zheng Z Y, Xu D Y, Dong W J. 2021. Extreme climate changes over three major river basins in China as seen in CMIP5 and CMIP6. *Climate Dynamics*, **57**, 1187–1205.

Guest Editor Tong Li
Managing Editor Lujuan Sun